# Low-temperature quasiparticle transport in a *d*-wave superconductor with coexisting charge order

Adam C. Durst[1] and Subir Sachdev[2]
[1]*Department of Physics and Astronomy, Stony Brook University, Stony Brook, New York 11794-3800, USA*
[2]*Department of Physics, Harvard University, Cambridge, Massachusetts 02138, USA*
(Received 21 October 2008; revised manuscript received 30 July 2009; published 26 August 2009)

In light of the evidence that charge order coexists with *d*-wave superconductivity in the underdoped cuprate superconductors, we investigate the manner in which such charge order will influence the quasiparticle excitations of the system and, in particular, the low-temperature transport of heat by those quasiparticles. We consider a d-wave superconductor in which the superconductivity coexists with charge density wave order of wave vector $(\pi/a,0)$. While the nodes of the quasiparticle energy spectrum survive the onset of charge order, there exists a critical value of the charge density wave order parameter beyond which the quasiparticle spectrum becomes fully gapped. We perform a linear response Kubo formula calculation of thermal conductivity in the low temperature (universal) limit. Results reveal the dependence of thermal transport on increasing charge order up to the critical value at which the quasiparticle spectrum becomes fully gapped and thermal conductivity vanishes. In addition to numerical results, closed-form expressions are obtained in the clean limit for the special case of isotropic Dirac nodes. Signatures of the influence of charge order on low-temperature thermal transport are identified.

DOI: 10.1103/PhysRevB.80.054518 PACS number(s): 74.72.−h, 74.25.Fy

## I. INTRODUCTION

The low energy quasiparticle excitations of the *d*-wave superconducting phase of the high-$T_c$ cuprate superconductors are massless anisotropic Dirac fermions.[1] These Dirac quasiparticles are easily excited in the vicinity of the four nodes, the four points on the two-dimensional Fermi surface where the superconducting order parameter vanishes. The dominant carriers of heat at low temperature, quasiparticles are efficiently probed via low temperature thermal conductivity measurements, which have been performed extensively over the past decade. Theory[2–8] has shown that the massless Dirac energy spectrum yields a low temperature limit where thermal conductivity is remarkably independent of disorder for small impurity density. In this limit, known as the universal limit, thermal conductivity per $CuO_2$ plane depends only on fundamental constants and the ratio of the Fermi velocity, $v_F$, to the *k*-space slope of the superconducting order parameter at the nodal points, $v_\Delta$. Experiments[9–18] have demonstrated this disorder independence and used this result to extract the anisotropy ratio, $\alpha \equiv v_F/v_\Delta$, from low-temperature thermal transport data.

Over the past few years, there has been significant effort to grow and measure high quality cuprate samples in the underdoped regime of the superconducting phase, as well as the pseudogap phase that results from underdoping even further. Several experimental groups have used high-resolution scanning tunneling microscopy[19–30] to examine the electronic states of the underdoped cuprates at the atomic scale. These experiments, among others,[31] have provided evidence that charge order coexists with *d*-wave superconductivity (dSC) in these materials. Furthermore, it has been shown theoretically[32–34] that coexisting charge order can significantly affect the quasiparticle spectrum of the superconductor, leading the system to become fully gapped for charge order of sufficient magnitude. If the quasiparticles are fully gapped (no nodes), the dominant carriers of heat at low temperature are frozen out, which should have a dramatic effect on the universal-limit thermal conductivity. Gusynin and Miransky[35] considered the effect of opening up a gap in the energy spectrum by explicitly adding a mass term to the Hamiltonian, and they showed that the zero-temperature thermal conductivity is thereby suppressed. In what follows, we add a charge order term to the Hamiltonian, show how the quasiparticle energy spectrum becomes fully gapped for sufficient charge order, and calculate the resulting zero-temperature thermal conductivity as a function of charge order, both before and after the nodes vanish.

We consider a particularly simple form of charge order, a conventional *s*-wave charge density wave (CDW) with a *k*-independent order parameter and a wave vector $\mathbf{Q}=(\pi/a,0)$ that doubles the unit cell. While the charge order in the underdoped cuprates may be of a more complex type, this simple model provides a place for us to start studying, phenomenologically, the effect of charge order on thermal transport in a *d*-wave superconductor. Furthermore, since the experimentally observed[22] CDW has a wave vector close to $(\pi/2a,0)$, it will generically have a second harmonic near $(\pi/a,0)$. This harmonic can couple efficiently to the nodal quasiparticles because its wave vector nearly spans the separation between the nodes.[36] The calculations presented in this paper can then be viewed as applying to this second harmonic.

While the charge order in the cuprates may turn on with underdoping, we simply add a CDW term to the dSC Hamiltonian and turn on the charge order by hand, by increasing the magnitude of the CDW order parameter. We then calculate the universal limit thermal conductivity of the combined system, evaluating the effect of coexisting charge order on thermal transport. Our goal is to identify signatures of the onset of charge order which may be observed with underdoping in low-temperature thermal conductivity measurements

 

of the underdoped cuprates. Evidence of the breakdown of universal thermal conductivity at low doping, possibly due to the onset of charge order, has already been seen experimentally,[37–42] and our results might therefore shed light on these studies.

We begin in Sec. II by writing down the combined Hamiltonian, calculating the resulting energy spectrum, and discussing the charge-order-induced transition whereby the spectrum can become fully gapped. In Sec. III, we calculate the Green's function and thermal current operator, define our model of disorder, and use a diagrammatic Kubo formula approach to obtain an integral form for the thermal conductivity tensor. For the special case of a clean system (no disorder) with isotropic nodes ($v_F = v_\Delta$) the remaining $k$-space integration can be performed analytically. This case is considered in Sec. IV where a closed-form solution is obtained for the thermal conductivity tensor as a function of the magnitude of the charge order. The more general case of nonzero disorder and anisotropic nodes is considered in Sec. V via a numerical computation, and the effect of disorder and nodal anisotropy is discussed. Conclusions are presented in Sec. VI.

## II. COEXISTING $d$ SC AND CDW ORDER

### A. Hamiltonian

Following Ref. 32, we consider a model Hamiltonian for a $d$-wave superconductor with coexisting charge order,

$$H = H_0 + H_{\mathrm{dSC}} + H_{\mathrm{CDW}}, \tag{1}$$

$$H_0 = \sum_{k\sigma} \epsilon_k c^\dagger_{k\sigma} c_{k\sigma}, \tag{2}$$

$$H_{\mathrm{dSC}} = \sum_k \Delta_k (c^\dagger_{k\uparrow} c^\dagger_{-k\downarrow} + c_{-k\downarrow} c_{k\uparrow}), \tag{3}$$

$$H_{\mathrm{CDW}} = \sum_{k\sigma} \psi c^\dagger_{k\sigma} c_{k+Q\sigma}. \tag{4}$$

Momenta are summed over the Brillouin zone of a two-dimensional square lattice of lattice constant $a$. $H_0 + H_{\mathrm{dSC}}$ is the mean-field BCS Hamiltonian for electron dispersion $\epsilon_k$ and superconducting order parameter $\Delta_k$, which is taken to have $d$-wave symmetry [for example, $\Delta_k = \Delta_0(\cos k_x a - \cos k_y a)/2$]. $H_{\mathrm{CDW}}$ denotes a charge density wave of wave vector $\mathbf{Q}$ with CDW order parameter $\psi$. While it is possible to consider density-wave states of nonzero angular momentum[43] by taking $\psi$ to be complex and $k$ dependent, we shall focus here on the effect of a conventional $s$-wave CDW corresponding to a site-centered charge modulation in the $x$ direction of wavelength twice the lattice constant. That is, we take $\psi$ to be a real, $k$-independent parameter and set $\mathbf{Q} = (\pi/a, 0)$.

The charge density wave has the effect of doubling the unit cell and therefore halving the effective Brillouin zone, as shown in Fig. 1. By defining a four-component extended-Nambu vector,

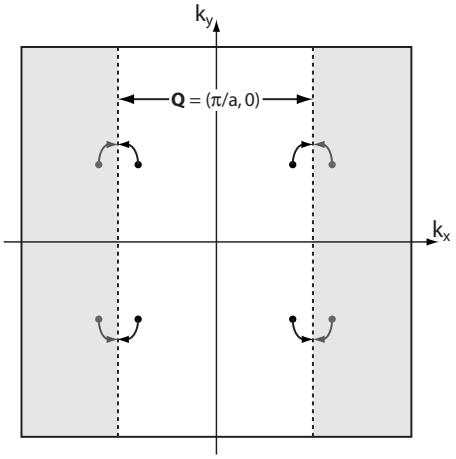


FIG. 1. Charge order of wave vector $\mathbf{Q} = (\pi/a, 0)$ doubles the unit cell and thereby halves the Brillouin zone. With increasing charge density wave order parameter, $\psi$, the nodes of the energy spectrum, and their images in the second reduced Brillouin zone (shaded), approach the reduced Brillouin zone edges (dotted), colliding for $\psi = \psi_c$, beyond which the spectrum is fully gapped.

$$\Psi^\dagger_k = [c^\dagger_{k\uparrow},\ c_{-k\downarrow},\ c^\dagger_{k+Q\uparrow},\ c_{-k-Q\downarrow}], \tag{5}$$

consisting of particle and hole operators at $\mathbf{k}$ and $\mathbf{k}+\mathbf{Q}$, we can express the Hamiltonian in a compact $4\times4$ matrix notation,

$$H = {\sum_k}' \Psi^\dagger_k H_k \Psi_k, \tag{6}$$

where

$$H_k = \begin{bmatrix} \epsilon_1 & \Delta_1 & \psi & 0 \\ \Delta_1 & -\epsilon_1 & 0 & -\psi \\ \psi & 0 & \epsilon_2 & \Delta_2 \\ 0 & -\psi & \Delta_2 & -\epsilon_2 \end{bmatrix}, \tag{7}$$

and subscript 1 denotes $\mathbf{k}$ and subscript 2 denotes $\mathbf{k}+\mathbf{Q}$. The prime indicates that the momentum sum is restricted to the reduced Brillouin zone. Note that the upper-left and lower-right $2\times2$ blocks of $H_k$ are simply the Nambu space Hamiltonian at $\mathbf{k}$ and $\mathbf{k}+\mathbf{Q}$ respectively. The CDW order parameter couples these two sectors.

### B. Energy spectrum and nodal collision

The energy spectrum of the fermionic excitations of this system of coexisting dSC and CDW order is obtained by solving for the (positive) eigenvalues of $H_k$. Doing so, we find that

$$E_k = \frac{1}{2}\{(\epsilon_1^2 + \Delta_1^2 + \epsilon_2^2 + \Delta_2^2 + 2\psi^2) \pm [(\epsilon_1^2 + \Delta_1^2 - \epsilon_2^2 - \Delta_2^2)^2 + 4\psi^2((\epsilon_1 + \epsilon_2)^2 + (\Delta_1 - \Delta_2)^2)]^{1/2}\}^{1/2}. \tag{8}$$

For $\psi = 0$, these solutions reduce to the energy spectra of the quasiparticle excitations of the $d$-wave superconductor, $E^0_k$ and $E^0_{k+Q}$, where $E^0_k = \sqrt{\epsilon_k^2 + \Delta_k^2}$. By construction, the quasipar-

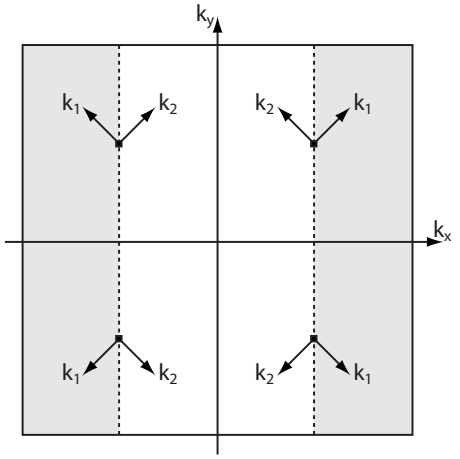


FIG. 2. Local coordinates, $k_1$ and $k_2$, defined about each of the four nodal collision points, $\mathbf{k}_c=(\pm\pi/2a,\pm\pi/2a)$. The $k_1$ axes, perpendicular to the Fermi surface, define the direction of increasing electron dispersion, $\epsilon_k$. The $k_2$ axes, parallel to the Fermi surface, define the direction of increasing superconducting order parameter, $\Delta_k$.

ticle energies drop to zero at four points in the Brillouin zone, the intersection of the Fermi surface with the lines $k_x=\pm k_y$. These are the nodal points, or nodes, of the $d$-wave superconductor. To model the situation in the cuprates, the nodes are taken to be a distance $k_F$ from the origin, inside of the $(\pm\pi/2a,\pm\pi/2a)$ points by a small distance $k_0$ where $k_0\equiv\pi/\sqrt{2}a-k_F\ll k_F$.

As the charge density wave is turned on, the nodal structure of the excitation spectrum initially survives, since the CDW wavevector, $\mathbf{Q}$, is not commensurate with the internodal distance.[32,36] With increasing $\psi$, the nodes move toward the reduced Brillouin zone edge along the trajectory sketched in Fig. 1. Also plotted in this figure is the trajectory of the image of each node translated by $\mathbf{Q}$ into the second reduced Brillouin zone. At a critical value of the CDW order parameter, $\psi=\psi_c$, the nodes collide at the reduced Brillouin zone edge and the energy spectrum becomes fully gapped. For $\psi>\psi_c$, the minimum values of the excitation spectra are nonzero. Hence, the nodes have vanished.

To determine the points in $k$ space at which this nodal collision occurs, we need only solve for the points at which a zero of $E_k$ coincides with a reduced Brillouin zone edge. We define the $\psi$ for which this occurs to be $\psi_c$. For example, node number 1 (located in the upper-right quadrant) will collide somewhere along the reduced zone boundary at $k_x=\pi/2a$. Setting $E(k_x=\pi/2a,k_y)=0$ and noting that both $\epsilon_k$ and $\Delta_k$ are even functions of $k_x$, we find that the collision point must satisfy $\epsilon_1=\epsilon_2=\psi_c$ and $\Delta_1=\Delta_2=0$. Near node number 1, the latter condition yields $k_x=k_y$, so the collision point is $\mathbf{k}_c=(\pi/2a,\pi/2a)$. Equivalent arguments for each of the four quadrants reveal that the four collision points are located at $(\pm\pi/2a,\pm\pi/2a)$. Defining local coordinates $k_1$ and $k_2$ about each of the collision points, as shown in Fig. 2, we can write

$$\epsilon_1=v_F(k_0+k_1)\quad \Delta_1=v_\Delta k_2,$$

$$\epsilon_2=v_F(k_0+k_2)\quad \Delta_2=v_\Delta k_1, \tag{9}$$

where $v_F$ is the Fermi velocity and $v_\Delta$ is the slope of the gap at the node. Note that in writing these linear relations, we have assumed that $k_0$ is small enough that the spectrum of the $d$-wave superconductor is still linear in the vicinity of the collision points. At the collision points $(k_1=k_2=0)$, $\epsilon_1=\epsilon_2=v_Fk_0$, which requires that $\psi_c=v_Fk_0$. Switching to scaled coordinates, $p_1\equiv\sqrt{v_Fv_\Delta}k_1$ and $p_2\equiv\sqrt{v_Fv_\Delta}k_2$, yields

$$\epsilon_1=\psi_c+\sqrt{\alpha}p_1\quad \Delta_1=p_2/\sqrt{\alpha},$$

$$\epsilon_2=\psi_c+\sqrt{\alpha}p_2\quad \Delta_2=p_1/\sqrt{\alpha}, \tag{10}$$

where $\alpha\equiv v_F/v_\Delta$. This notation provides a convenient framework with which to proceed with the thermal transport calculation.

## III. TRANSPORT CALCULATION

Given the Hamiltonian defined by Eqs. (7) and (10), we can calculate the thermal conductivity, and its dependence on the charge density wave order parameter, via Kubo formula.

### A. Green's function

We begin by computing the Matsubara Green's function. In the extended-Nambu basis of Eq. (5), the bare Green's function is a $4\times4$ matrix obtained through inversion of the Hamiltonian

$$G^0(k,i\omega)=[i\omega-H_k]^{-1}. \tag{11}$$

It takes the form

$$G^0(k,\omega)=\frac{1}{G_{\rm den}}\begin{bmatrix}G_a & G_b\\ G_c & G_d\end{bmatrix}, \tag{12}$$

$$G_a=((i\omega)^2-\epsilon_2^2-\Delta_2^2)[i\omega+\epsilon_1\tau_3+\Delta_1\tau_1]-\psi^2[i\omega-\epsilon_2\tau_3+\Delta_2\tau_1], \tag{13}$$

$$G_b=\psi[i\omega(\epsilon_1+\epsilon_2)+((i\omega)^2+\epsilon_1\epsilon_2-\Delta_1\Delta_2-\psi^2)\tau_3+(\epsilon_1\Delta_2+\epsilon_2\Delta_1)\tau_1-i\omega(\Delta_1-\Delta_2)(i\tau_2)], \tag{14}$$

$$G_c=\psi[i\omega(\epsilon_1+\epsilon_2)+((i\omega)^2+\epsilon_1\epsilon_2-\Delta_1\Delta_2-\psi^2)\tau_3+(\epsilon_1\Delta_2+\epsilon_2\Delta_1)\tau_1+i\omega(\Delta_1-\Delta_2)(i\tau_2)], \tag{15}$$

$$G_d=((i\omega)^2-\epsilon_1^2-\Delta_1^2)[i\omega+\epsilon_2\tau_3+\Delta_2\tau_1]-\psi^2[i\omega-\epsilon_1\tau_3+\Delta_1\tau_1], \tag{16}$$

$$G_{\rm den}=(\epsilon_1^2+\Delta_1^2+\psi^2-(i\omega)^2)(\epsilon_2^2+\Delta_2^2+\psi^2-(i\omega)^2)-\psi^2((\epsilon_1+\epsilon_2)^2+(\Delta_1-\Delta_2)^2), \tag{17}$$

where $G_{\rm den}$ is a scalar and $G_a$, $G_b$, $G_c$, and $G_d$ are $2\times2$ matrices expressed in terms of particle-hole-space Pauli matrices, $\tau_i$.

In the presence of disorder, we must include the impurity contribution to the self-energy via Dyson's equation

$$G^{-1} = G^{0-1} - \Sigma. \tag{18}$$

The self-energy, $\Sigma$, is a $4\times4$ matrix in the extended-Nambu basis, but for simplicity, we consider here only the scalar term

$$\Sigma = \Sigma(i\omega)\mathbb{1} \tag{19}$$

and postpone discussion of the effects of off-diagonal self-energy terms to a separate publication.[44] Then the dressed Matsubara Green's function is simply

$$G(k,i\omega) = [(i\omega - \Sigma(i\omega))\mathbb{1} - H_k]^{-1} = G^0(k, i\omega - \Sigma(i\omega)). \tag{20}$$

For our calculation of the zero-temperature thermal conductivity, we will require only the imaginary part of the zero-frequency retarded Green's function, Im $G^R(k,\omega\to0)$. Continuing $i\omega\to\omega+i\delta$ and taking the $\omega\to0$ limit, the zero-frequency retarded self-energy is just a negative imaginary constant, $-i\Gamma_0$, and we find that

$$\text{Im } G^R(k,\omega\to0) = \frac{1}{G_{\text{den}}}\begin{bmatrix} G''_a & G''_b \\ G''_c & G''_d \end{bmatrix}, \tag{21}$$

$$G''_a = -\Gamma_0(\Gamma_0^2 + \psi^2 + \epsilon_2^2 + \Delta_2^2), \tag{22}$$

$$G''_b = \psi\Gamma_0[(\epsilon_1+\epsilon_2) - (\Delta_1-\Delta_2)(i\tau_2)], \tag{23}$$

$$G''_c = \psi\Gamma_0[(\epsilon_1+\epsilon_2) + (\Delta_1-\Delta_2)(i\tau_2)], \tag{24}$$

$$G''_d = -\Gamma_0(\Gamma_0^2 + \psi^2 + \epsilon_1^2 + \Delta_1^2), \tag{25}$$

$$G_{\text{den}} = (\Gamma_0^2+\psi^2+\epsilon_1^2+\Delta_1^2)(\Gamma_0^2+\psi^2+\epsilon_2^2+\Delta_2^2) - \psi^2((\epsilon_1+\epsilon_2)^2 + (\Delta_1-\Delta_2)^2), \tag{26}$$

where $\Gamma_0$ is the zero-frequency impurity scattering rate (the impurity-induced broadening of the spectral function).

### B. Current operator

Next we must calculate the quasiparticle current operator for this system of coexisting $d$-wave superconductor and charge order. We note that quasiparticles carry a well-defined heat and spin. Thus, where a quasiparticle goes, so goes its heat and spin. Though the quantity we require is the thermal current, we will proceed by calculating the spin current operator (which is technically simpler) obtaining the thermal current operator by correspondence.

The spin current operator, $\mathbf{j}^s$, is obtained via continuity with the spin density operator, $\rho^s$,

$$-\nabla\cdot\mathbf{j}^s = \rho^s = \frac{1}{i}[\rho^s, H]. \tag{27}$$

Fourier transforming and taking the zero-wavevector limit yield a recipe for calculating $\mathbf{j}^s_{q=0}$, which is the operator we will need for the transport calculation,

$$\mathbf{q}\cdot\mathbf{j}^s_0 = \lim_{q\to0}[\rho^s_q, H]. \tag{28}$$

Defining and re-expressing the spin density operator in various forms, we note that

$$\rho^s_q \equiv \sum_{k'\sigma} S_\sigma c^\dagger_{k'\sigma} c_{k'+q\sigma} = s{\sum_{k'}}' \Psi^\dagger_{k'}\Psi_{k'+q}$$
$$= s{\sum_{k'}}' (c^\dagger_{k'\uparrow}c_{k'+q\uparrow} + c_{-k'\downarrow}c^\dagger_{-k'-q\downarrow} + d^\dagger_{k'\uparrow}d_{k'+q\uparrow} + d_{-k'\downarrow}d^\dagger_{-k'-q\downarrow}), \tag{29}$$

where $S_\sigma = \pm s$, $s=1/2$, $d_{k\sigma}\equiv c_{k+Q\sigma}$, $\Psi_k$ is the four-component extended-Nambu vector defined in Eq. (5), and the prime restricts the wave vector sum to the reduced Brillouin zone. In the same notation, the Hamiltonian takes the form

$$H = {\sum_k}' \Psi^\dagger_k H_k \Psi_k = {\sum_k}' [\epsilon_k(c^\dagger_{k\uparrow}c_{k\uparrow} - c_{-k\downarrow}c^\dagger_{-k\downarrow}) + \Delta_k(c^\dagger_{k\uparrow}c^\dagger_{-k\downarrow} + c_{-k\downarrow}c_{k\uparrow}) + \epsilon_{k+Q}(d^\dagger_{k\uparrow}d_{k\uparrow} - d_{-k\downarrow}d^\dagger_{-k\downarrow}) + \Delta_{k+Q}(d^\dagger_{k\uparrow}d^\dagger_{-k\downarrow} + d_{-k\downarrow}d_{k\uparrow}) + \psi(c^\dagger_{k\uparrow}d_{k\uparrow} - c_{-k\downarrow}d^\dagger_{-k\downarrow} + d^\dagger_{k\uparrow}c_{k\uparrow} - d_{-k\downarrow}c^\dagger_{-k\downarrow})]. \tag{30}$$

Using fermion anticommutation relations to evaluate the commutator in Eq. (28), we find that

$$\mathbf{j}^s_0 = s{\sum_k}' \Psi^\dagger_k \begin{bmatrix} \mathbf{v}_{Fk}\tau_3 + \mathbf{v}_{\Delta k}\tau_1 & \mathbf{v}_{\psi k}\tau_3 \\ \mathbf{v}_{\psi k}\tau_3 & \mathbf{v}_{Fk+Q}\tau_3 + \mathbf{v}_{\Delta k+Q}\tau_1 \end{bmatrix} \Psi_{k+Q}, \tag{31}$$

where $\mathbf{v}_{Fk}\equiv\partial\epsilon_k/\partial\mathbf{k}$, $\mathbf{v}_{\Delta k}\equiv\partial\Delta_k/\partial\mathbf{k}$, and $\mathbf{v}_{\psi k}\equiv\partial\psi/\partial\mathbf{k}$. For the case we consider, $\psi$ is $k$-independent, so $\mathbf{v}_{\psi k}$ is precisely zero and the spin current operator is block diagonal in the extended-Nambu basis.

In the vicinity of each of the four collision points (the regions we will always be considering), $\mathbf{v}_{Fk}$ points along the locally defined $k_1$ direction and $\mathbf{v}_{\Delta k}$ points along the locally defined $k_2$-direction, as shown in Fig. 2. Therefore, shifting by wave vector $\mathbf{Q}=(\pi/a,0)$ from $\mathbf{k}$ to $\mathbf{k}+\mathbf{Q}$ flips the sign of the $x$ component of each velocity while preserving the $y$ component. That is, the components satisfy $v^i_{Fk+Q} = \eta_i v^i_{Fk}$ and $v^i_{\Delta k+Q} = \eta_i v^i_{\Delta k}$ for

$$\eta_i \equiv \begin{Bmatrix} -1 & \text{for} & i=x \\ +1 & \text{for} & i=y \end{Bmatrix}, \tag{32}$$

so we can write

$$\mathbf{j}^s_0 = s{\sum_k}' \Psi^\dagger_k[\mathbf{v}_{MF} + \mathbf{v}_{M\Delta}]\Psi_{k+Q}, \tag{33}$$

where

$$\mathbf{v}_{MF} \equiv v^x_{Fk}M^x_3\hat{\mathbf{x}} + v^y_{Fk}M^y_3\hat{\mathbf{y}}, \tag{34}$$

$$\mathbf{v}_{M\Delta} \equiv v^x_{\Delta k}M^x_1\hat{\mathbf{x}} + v^y_{\Delta k}M^y_1\hat{\mathbf{y}}, \tag{35}$$

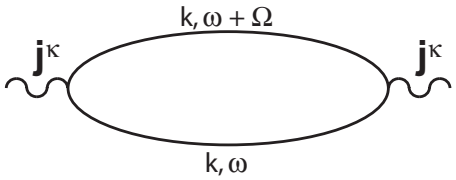


FIG. 3. Feynman diagram depicting the bare bubble thermal current-current correlation function, $\vec{\vec{\Pi}}_\kappa(i\Omega)$. The thermal current operator sits on each vertex and each propagator denotes a Green's function dressed with disorder self-energy.

$$M_3^i \equiv \begin{pmatrix} \tau_3 & 0 \\ 0 & \eta_i \tau_3 \end{pmatrix} \quad M_1^i \equiv \begin{pmatrix} \tau_1 & 0 \\ 0 & \eta_i \tau_1 \end{pmatrix}. \tag{36}$$

Finally, we note that since the same quasiparticles that carry the spin also carry the heat, the thermal current operator, $\mathbf{j}^\kappa$, will have the same structure as the spin current operator. In the zero-wave-vector, zero-frequency limit that we will require,

$$\mathbf{j}_0^\kappa = \lim_{q,\Omega\to 0} {\sum_{k\omega}}' \left(\omega + \frac{\Omega}{2}\right) \Psi_{k,\omega}^\dagger [\mathbf{v}_{MF} + \mathbf{v}_{M\Delta}] \Psi_{k+Q,\omega+\Omega}. \tag{37}$$

### C. Thermal conductivity

Given the Green's function, thermal current operator, and coordinate system defined in the previous sections, we can calculate the thermal conductivity via the Kubo formula[45]

$$\frac{\vec{\kappa}(T)}{T} = -\lim_{\Omega\to 0} \frac{\mathrm{Im}\, \vec{\vec{\Pi}}_\kappa^R(\Omega)}{T^2 \Omega}, \tag{38}$$

where the retarded current-current correlation function is obtained from the Matsubara function via analytic continuation,

$$\vec{\vec{\Pi}}_\kappa^R(\Omega) = \vec{\vec{\Pi}}_\kappa(i\Omega \to \Omega + i\delta). \tag{39}$$

In what follows, we neglect vertex corrections, calculating the bare bubble current-current correlation function using the Matsubara formalism.[45] It has been shown previously[8] that vertex corrections are negligible for the $d$-wave superconductor case (without charge order) and the contribution of vertex corrections to the present case will be considered in a separate paper.[44]

Evaluating the bare bubble Feynman diagram shown in Fig. 3 yields

$$\vec{\vec{\Pi}}_\kappa(i\Omega) = \frac{1}{\beta} \sum_{i\omega} {\sum_k}' \left(i\omega + \frac{i\Omega}{2}\right)^2 \mathrm{Tr}[G(k,i\omega)\mathbf{v}_M G(k, i\omega + i\Omega)\mathbf{v}_M], \tag{40}$$

where $\mathbf{v}_M \equiv \mathbf{v}_{MF} + \mathbf{v}_{M\Delta}$ is a vector in coordinate space and a matrix in extended-Nambu space, the Green's functions are dressed with disorder, the $\omega$ sum is over fermionic Matsubara frequencies, the $k$-sum is restricted to the first reduced Brillouin zone, the trace is over extended-Nambu space, and $\beta = 1/k_B T$. We expand the $k$-sum from the reduced Brillouin zone to the full (original) Brillouin zone, which double-counts and therefore requires division by 2. Since the summand is sharply peaked in the vicinity of the four nodal collision points, we then replace the $k$-sum by four integrals over local scaled coordinates, $p_1$ and $p_2$, defined (in Sec. II B) about each of these points,

$$\sum_k \to \frac{1}{2}\sum_k \to \frac{1}{2}\sum_{j=1}^4 \int \frac{d^2p}{(2\pi)^2 v_F v_\Delta}. \tag{41}$$

Making use of a spectral representation of the matrix Green's function

$$G(\mathbf{p}, i\omega) = \int d\omega_1 \frac{-\frac{1}{\pi}\mathrm{Im}\, G^R(\mathbf{p},\omega_1)}{i\omega - \omega_1}. \tag{42}$$

Equation (40) becomes

$$\vec{\vec{\Pi}}_\kappa(i\Omega) = \frac{1}{2\pi^2 v_F v_\Delta} \int \frac{d^2p}{(2\pi)^2} \int d\omega_1 d\omega_2 S(i\Omega) \mathrm{Tr} \times \left[\sum_{j=1}^4 G_R''(\mathbf{p},\omega_1)\mathbf{v}_M^{(j)} G_R''(\mathbf{p},\omega_2)\mathbf{v}_M^{(j)}\right], \tag{43}$$

where

$$S(i\Omega) = \frac{1}{\beta}\sum_{i\omega} \left(i\omega + \frac{i\Omega}{2}\right)^2 \frac{1}{i\omega - \omega_1} \frac{1}{i\omega + i\Omega - \omega_2} \tag{44}$$

and $\mathbf{v}_M^{(j)}$ is the value of $\mathbf{v}_M$ in the vicinity of collision point $j$. (Note that while the spectral representation defined in Eq. (42) is valid for the case of real $\psi$ that we are considering, it would not be valid if $\psi$, and therefore $H_k$, was complex. The subtleties of this are discussed in detail in the Appendix.)

Computing the Matsubara sum in Eq. (44) via contour integration (see Refs. 8 and 46 for discussion of technical points), continuing $i\Omega \to \Omega + i\delta$ to obtain the retarded function, and taking the imaginary part, we find that

$$S_R''(\Omega) = \pi\left(\omega_1 + \frac{\Omega}{2}\right)^2 (n_F(\omega_1 + \Omega) - n_F(\omega_1))\delta(\omega_1 + \Omega - \omega_2), \tag{45}$$

where $n_F(x) = 1/(e^{\beta x} + 1)$ is the Fermi function the double-prime indicates the imaginary part. Then taking the $\Omega \to 0$ limit in Eq. (38) yields an expression for the thermal conductivity tensor

$$\frac{\vec{\kappa}(T)}{T} = \frac{-1}{2\pi^2 v_F v_\Delta} \int d\omega \left(\frac{\omega}{T}\right)^2 \frac{\partial n_F}{\partial \omega} \int \frac{d^2p}{4\pi} \mathrm{Tr}\, \vec{R}(\mathbf{p},\omega), \tag{46}$$

where

$$\vec{R}(\mathbf{p},\omega) = \sum_{j=1}^4 G_R''(\mathbf{p},\omega_1)\mathbf{v}_M^{(j)} G_R''(\mathbf{p},\omega_2)\mathbf{v}_M^{(j)} \tag{47}$$

and taking the $T \to 0$ limit yields

$$\frac{\overleftrightarrow{\kappa}_0}{T} = \frac{k_B^2}{6v_F v_\Delta}\int \frac{d^2p}{4\pi} \mathrm{Tr}\, \overleftrightarrow{R}(\mathbf{p},0). \tag{48}$$

Here we have used the fact that, for low $T$, $(\omega/T)^2(-\partial n_F/\partial\omega)$ is sharply peaked at $\omega=0$ and

$$\int_{-\infty}^{\infty} d\omega \left(\frac{\omega}{T}\right)^2 \left(-\frac{\partial n_F}{\partial \omega}\right) = \frac{\pi^2 k_B^2}{3}. \tag{49}$$

Noting that at each collision point, $\mathbf{v}_F$ and $\mathbf{v}_\Delta$ point along the local $k_1$ and $k_2$ directions respectively (as defined in Fig. 2) and performing the sum over collision points in Eq. (47), we find that

$$R_{ii}(\mathbf{p},0) = 2v_F^2 G_R'' M_3^i G_R'' M_3^i + 2v_\Delta^2 G_R'' M_1^i G_R'' M_1^i + 2\eta_i v_F v_\Delta (G_R'' M_3^i G_R'' M_1^i + G_R'' M_1^i G_R'' M_3^i) \tag{50}$$

for $i=\{x,y\}$ while

$$R_{xy}(\mathbf{p},0) = R_{yx}(\mathbf{p},0) = 0, \tag{51}$$

where $\eta_i$, $M_3^i$, and $M_1^i$ are defined in Eqs. (32) and (36). Plugging in the Green's function from Eqs. (21)–(26) and taking the trace over the $4\times4$ extended-Nambu space yields

$$\frac{\kappa_0^{ii}}{T} = \frac{\kappa_{00}}{T}\int \frac{d^2p}{4\pi}\frac{N_1+\eta_i N_2}{D}, \tag{52}$$

$$N_1 = 2A[(A+B+\epsilon_1^2+\Delta_1^2)^2 + (A+B+\epsilon_2^2+\Delta_2^2)^2], \tag{53}$$

$$N_2 = 4AB[(\epsilon_1+\epsilon_2)^2 - (\Delta_1-\Delta_2)^2], \tag{54}$$

$$D = [(A+B+\epsilon_1^2+\Delta_1^2)(A+B+\epsilon_2^2+\Delta_2^2) - B((\epsilon_1+\epsilon_2)^2 + (\Delta_1-\Delta_2)^2)]^2, \tag{55}$$

where

$$\frac{\kappa_{00}}{T} \equiv \frac{k_B^2}{3\hbar}\left(\frac{v_F}{v_\Delta}+\frac{v_\Delta}{v_F}\right) \tag{56}$$

is the universal-limit thermal conductivity for a $d$-wave superconductor (without charge order) and we have defined $A \equiv \Gamma_0^2$ (our parameter of disorder) and $B \equiv \psi^2$ (our parameter of charge order). Inserting our expressions for the $\epsilon$'s and $\Delta$'s from Eq. (10) and integrating over $\mathbf{p}$, we can obtain the zero-temperature thermal conductivity as a function of $\psi$, $\Gamma_0$, and $\alpha=v_F/v_\Delta$. We expect these results, calculated in the zero-temperature limit, to apply within a regime where temperature is small compared to all other energy scales in the problem. Estimating the extent of this regime, which likely depends on the details of the disorder[6] and charge order, would require the calculation of nonzero-temperature corrections and is beyond the scope of this paper.

## IV. ANALYTICAL RESULTS: CLEAN ISOTROPIC LIMIT

In the clean $(A=\Gamma_0^2\to0)$, isotropic $(\alpha=v_F/v_\Delta=1)$ limit, the integrals in Eq. (52) can be performed analytically, providing us with a closed-form expression for the thermal conductivity tensor as a function of the charge density wave order parameter, $\psi$. Selecting $\psi_c$ (the value of $\psi$ at which the nodes vanish) as our energy unit, and for $\alpha=1$, Eq. (10) becomes

$$\epsilon_1 = p_1+1 \quad \Delta_1 = p_2,$$

$$\epsilon_2 = p_2+1 \quad \Delta_2 = p_1. \tag{57}$$

It is then useful to make a change of variables to

$$q_1 \equiv p_1 - p_2,$$

$$q_2 \equiv p_1 + p_2 + 1 \tag{58}$$

such that

$$\epsilon_1 = (q_1+q_2+1)/2 \quad \Delta_1 = (q_2-q_1-1)/2,$$

$$\epsilon_2 = (q_2-q_1+1)/2 \quad \Delta_2 = (q_1+q_2-1)/2. \tag{59}$$

Note that this change of variables has a Jacobian of 1/2 such that $\int d^2p \to \frac{1}{2}\int d^2q$. Therefore,

$$\frac{\kappa_0^{ii}}{\kappa_{00}} = \int \frac{d^2q}{8\pi}\frac{N_1+\eta_i N_2}{D}, \tag{60}$$

$$N_1 = 4A\left[\left(A+B+\frac{q^2+1}{2}\right)^2 + q_1^2\right], \tag{61}$$

$$N_2 = 4AB[(q_2+1)^2 - q_1^2], \tag{62}$$

$$D = [f + A(q^2+1+2B) + A^2]^2, \tag{63}$$

where

$$f = \frac{(q^2-1)^2}{4} + (q_2-B)^2. \tag{64}$$

In the $A\to0$ limit, the numerator vanishes, so contributions to the integral come only from the vicinity of points in $q$-space where the denominator vanishes as well, which requires $f=0$. It is clear from Eq. (64) that $f$ is only equal to zero when $q=1$ and $q_2=B$, the intersection of a unit circle about the origin and a horizonal line at $q_2=B$.

For $B>1$, there is no intersection, so the integral is zero. This is quite physical, since for $B>1$, $\psi>\psi_c$ and the energy spectrum is gapped. Thus, in the clean, zero-temperature limit, there are no quasiparticles to transport heat and the thermal conductivity is zero.

For $B<1$, the circle and line intersect at two points, $\mathbf{q}_n = (\pm\sqrt{1-B^2}, B)$. These points are precisely the node and ghost node of the energy spectrum, which will collide when $\psi$ reaches $\psi_c$. For vanishing $A$, terms in $N_1$, $N_2$, and $D$ that are higher than first order in $A$ can be safely neglected and terms first order in $A$ can be replaced by their values at $\mathbf{q}=\mathbf{q}_n$. Doing so, we find that

$$\frac{\kappa_0^{ii}}{\kappa_{00}} = (1+\eta_i B^2)8(1+B)I_1, \tag{65}$$

where

$$I_1 \equiv \int \frac{d^2q}{8\pi} \frac{A}{[f+2A(1+B)]^2} \tag{66}$$

and $f$ is the function of $\mathbf{q}$ given in Eq. (64). Changing variables to

$$x_1 \equiv q_1 - 1 = x\cos\theta,$$

$$x_2 \equiv q_2 = x\sin\theta, \tag{67}$$

we see that

$$\begin{aligned} f &= x^4/4 + B^2 + x^2 + x^3\cos\theta - 2Bx\sin\theta \\ &= \frac{x^2}{h^2}[1+h^2+2h(\cos\theta\cos\theta_0 - \sin\theta\sin\theta_0)] \\ &= \frac{x^2}{h^2}[1+h^2+2h\cos(\theta+\theta_0)] \end{aligned} \tag{68}$$

where

$$h \equiv \frac{x}{\sqrt{x^4/4+B^2}} \quad \text{and} \quad \tan\theta_0 \equiv \frac{2B}{x^2}. \tag{69}$$

Then plugging $f$ into Eq. (66), shifting $\theta \to \theta - \theta_0 + \pi$, and defining $\gamma \equiv 2(1+B)h^2/x^2$, we find that

$$\begin{aligned} I_1 &= \frac{1}{8\pi}\int_0^\infty dx x \int_{-\pi}^{\pi} d\theta \frac{h^4}{x^4}\frac{A}{[1+h^2-2h\cos\theta+A\gamma]^2} \\ &= \frac{1}{8\pi(1+B)}\int_0^\infty \frac{dx}{x} h^2 I_2 \end{aligned} \tag{70}$$

where

$$I_2 \equiv \int_0^\pi d\theta \frac{A\gamma}{[1+h^2+A\gamma-2h\cos\theta]^2}. \tag{71}$$

This integral over $\theta$ is standard and easily evaluated via integration table.[47] Doing so yields

$$I_2 = 2\pi\frac{1+h^2}{(1+h)^3} D(h-1, A\gamma) \tag{72}$$

where

$$D(u,\Gamma) \equiv \frac{\Gamma^2/2}{(u^2+\Gamma^2)^{3/2}}. \tag{73}$$

Since $\gamma$ is finite for all $x$, $A\gamma$ vanishes as $A \to 0$. Therefore, noting that

$$\lim_{\Gamma\to 0} D(u,\Gamma) = \begin{cases} 0 & \text{for} \quad u \neq 0 \\ \infty & \text{for} \quad u = 0 \end{cases} \tag{74}$$

and

$$\int_{-\infty}^{\infty} du D(u,\Gamma) = 1 \tag{75}$$

we see that $D(u, \Gamma \to 0)$ is a representation of the Dirac delta function. Hence,

$$I_2 = \frac{\pi}{2}\delta(h-1) \tag{76}$$

and

$$I_1 = \frac{1}{16(1+B)}\int_0^\infty dx \frac{x}{x^4/4+B^2}\delta(h-1). \tag{77}$$

Noting that $\delta(h-1) = 2\delta(h^2-1)$ (since $h>1$) and letting $u \equiv x^2/2$, this becomes

$$I_1 = \frac{1}{8(1+B)}\int_0^\infty \frac{du}{u^2+B^2}\delta\left(\frac{2u}{u^2+B^2} - 1\right). \tag{78}$$

For $B>1$, the argument of the delta function is never zero, so $I_1=0$, as expected. For $B<1$, the argument is zero at two points, $u=u_\pm = 1 \pm \sqrt{1-B^2}$, so after a bit of delta-function gymnastics, we find that

$$\begin{aligned} I_1 &= \frac{1}{16(1+B)}\frac{1}{\sqrt{1-B^2}}\int_0^\infty du[\delta(u-u_-)+\delta(u-u_+)] \\ &= \frac{1}{8(1+B)}\frac{\Theta(1-B)}{\sqrt{1-B^2}} \end{aligned} \tag{79}$$

where $\Theta(x)$ is the Heaviside step function. Finally, plugging back into Eq. (65), we obtain a very simple closed-form expression for the zero-temperature thermal conductivity tensor in the clean isotropic limit.

$$\frac{\kappa_0^{xx}}{\kappa_{00}} = \sqrt{1-(\psi/\psi_c)^4}\,\Theta(\psi_c-\psi), \tag{80}$$

$$\frac{\kappa_0^{yy}}{\kappa_{00}} = \frac{1+(\psi/\psi_c)^4}{\sqrt{1-(\psi/\psi_c)^4}}\Theta(\psi_c-\psi), \tag{81}$$

$$\kappa_0^{xy} = \kappa_0^{yx} = 0. \tag{82}$$

These results are plotted in Fig. 4. For $\psi=0$, we recover the universal-limit thermal conductivity of a $d$-wave superconductor[8] [see Eq. (56)]. And for $\psi > \psi_c$, as expected, the thermal conductivity vanishes since the system has become gapped and there are no quasiparticles to transport the heat. For $\psi$ between zero and $\psi_c$, thermal transport in the $x$ and $y$ directions differ, which makes sense as square symmetry has been explicitly broken by the charge density wave oriented in the $x$ direction. Parallel to the CDW wave vector, thermal conductivity in the $x$-direction decreases monotonically with $\psi$, vanishing continuously at $\psi_c$. Perpendicular to the CDW wave vector, thermal conductivity in the $y$-direction increases with $\psi$, exhibiting a square-root divergence before vanishing abruptly at $\psi_c$. This divergence, a consequence of the clean limit, is replaced by a peak in $\kappa_0^{yy}$ when nonzero disorder is considered, as will be shown in the next section.

## V. NUMERICAL RESULTS

For the general case of nonzero disorder ($\Gamma_0 \neq 0$) and/or anisotropic Dirac nodes ($\alpha = v_F/v_\Delta \neq 1$), the $p$-space integra-

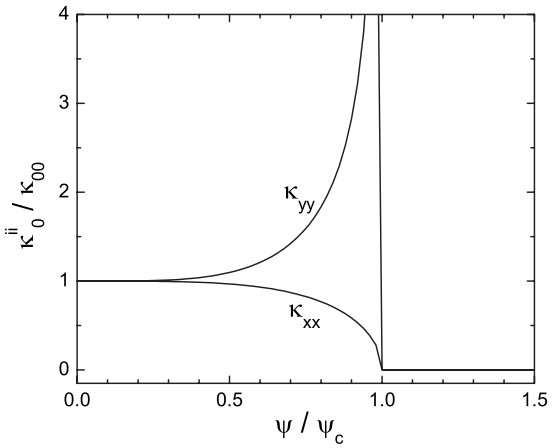


FIG. 4. Calculated zero-temperature thermal conductivity tensor in the clean ($\Gamma_0 \to 0$), isotropic ($v_F = v_\Delta$) limit. We plot $\kappa_0^{xx}$ and $\kappa_0^{yy}$ as functions of the charge density wave order parameter, $\psi$, from the closed-form expressions in Eqs. (80) and (81). As $\psi$ approaches $\psi_c$, the value beyond which the quasiparticle spectrum becomes gapped, $\kappa_0^{xx}$ vanishes continuously while $\kappa_0^{yy}$ diverges before dropping to zero.

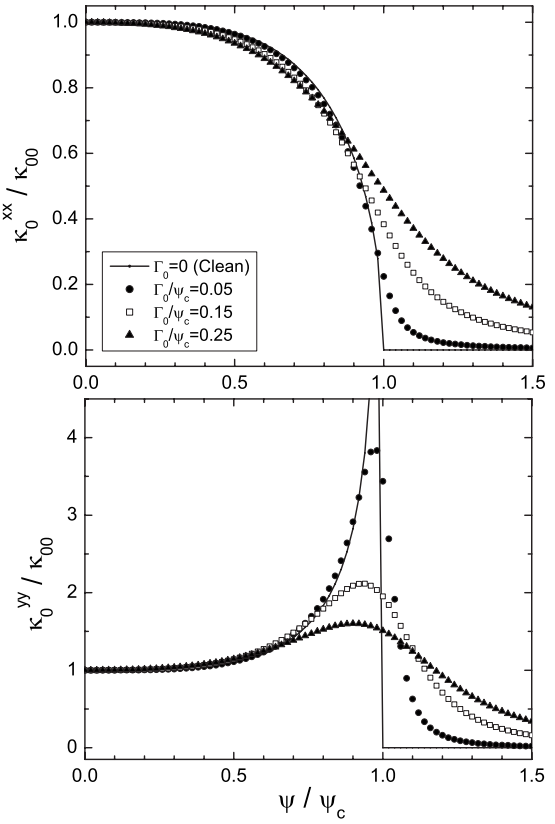


FIG. 5. Disorder dependence of calculated zero-temperature thermal conductivity tensor. We plot $\kappa_0^{xx}$ (upper panel) and $\kappa_0^{yy}$ (lower panel) as functions of charge density wave order parameter, $\psi$, for several values of the disorder parameter, $\Gamma_0$. In all cases, $\alpha = v_F/v_\Delta = 1$. Included for comparison is the clean limit result (solid lines). Note that disorder smoothes the transition to zero thermal conductivity that results from the gapping of the energy spectrum at $\psi = \psi_c$. The divergence of $\kappa_0^{yy}$ seen in the clean case is replaced by a peak that is diminished and broadened with increasing disorder.

tion in Eq. (52) is more complicated, but can be computed numerically. Doing so, we calculated the zero-temperature thermal conductivity tensor as a function of charge density wave order parameter, $\psi$, our parameter of disorder, $\Gamma_0$, and the anisotropy of the Dirac nodes, $\alpha = v_F/v_\Delta$. Results are plotted in Figs. 5 and 6.

Figure 5 shows $\kappa_0^{xx}$ and $\kappa_0^{yy}$ as functions of $\psi$ for several values of $\Gamma_0$ and $\alpha = 1$. The clean-limit results calculated in Sec. IV are included (solid lines) for comparison. Note that as disorder increases, the transition to zero thermal conductivity at the nodal collision point ($\psi = \psi_c$) gets rounded out, and the peak in $\kappa_0^{yy}$ just prior to the collision point is diminished and broadened. Essentially, and not unexpectedly, disorder blurs the nodal collision, smoothing out the sharp transition seen in the clean case.

The $\Gamma_0 = 0.05\psi_c$ results are reproduced in Fig. 6, along with plots of $\kappa_0^{xx}$ and $\kappa_0^{yy}$ versus $\psi$ for larger values of $\alpha$. For constant disorder, increasing $\alpha$ changes the shape of the $\kappa_0^{xx}$ curve and diminishes and broadens the peak in $\kappa_0^{yy}$. The effect of increased nodal anisotropy is similar to, but distinct from, that of disorder, further smoothing the transition to zero thermal conductivity that occurs abruptly at $\psi = \psi_c$ in the clean, isotropic case.

Note that in the presence of disorder, since the thermal conductivity does not drop abruptly to zero at $\psi = \psi_c$, there exists a range of $\psi$ over which the zero-temperature thermal conductivity is nonzero despite the fact that the energy spectrum has become fully gapped.

## VI. CONCLUSIONS

The coexistence of $d$-wave superconductivity with charge order of sufficient magnitude can have a significant effect on the energy spectrum of the Bogoliubov quasiparticles and the transport of heat by those quasiparticles at low temperatures. In this paper, we have considered a particularly simple form of charge order, a conventional $s$-wave charge density wave of wave vector $\mathbf{Q} = (\pi/a, 0)$, the magnitude of which is characterized by a real, $k$-independent order parameter, $\psi$. The charge order halves the Brillouin zone, and as a function of $\psi$, the four nodes of the quasiparticle energy spectrum move in $k$ space, approaching the reduced Brillouin zone edge. When $\psi$ reaches $\psi_c$, equal to the Fermi velocity times the $k$-space distance from the original node location to the $(\pi/2, \pi/2)$ point, the nodes reach the reduced Brillouin zone edge and collide with their counterparts in the second reduced Brillouin zone. Beyond this point, the nodes vanish and the quasiparticle energy spectrum is fully gapped.

We have used a linear response Kubo formula approach to calculate the zero temperature limit of the thermal conductivity tensor for this system. Working within an extended-Nambu basis (particle, hole, particle shifted by $\mathbf{Q}$, hole shifted by $\mathbf{Q}$), we constructed a $4 \times 4$ matrix Hamiltonian, Green's function, and thermal current operator. We then used the Matsubara technique to evaluate the bare-bubble thermal current-current correlator, neglecting vertex corrections and including disorder in the self-energy via a single broadening parameter, $\Gamma_0$. From this we calculated $\kappa^{xx}/T$ and $\kappa^{yy}/T$, in

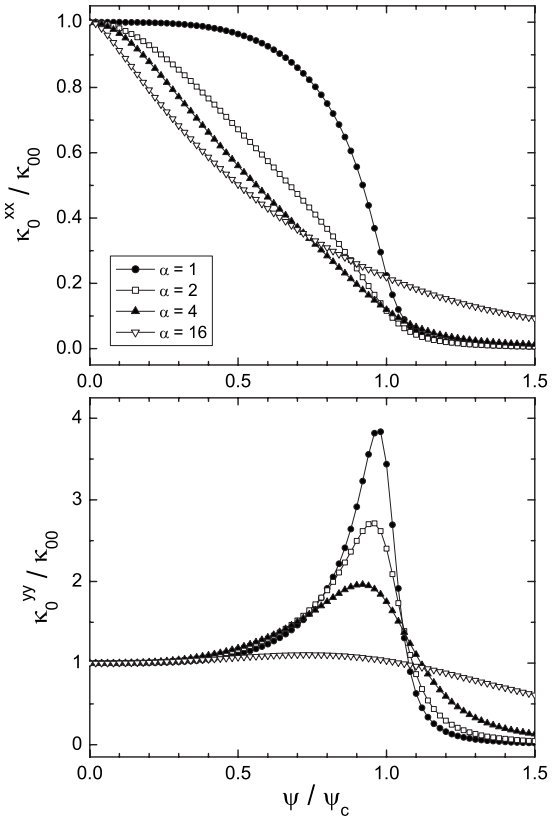


FIG. 6. Nodal anisotropy dependence of calculated zero-temperature thermal conductivity tensor. For fixed disorder ($\Gamma_0 = 0.05\psi_c$), we plot $\kappa_0^{xx}$ (upper panel) and $\kappa_0^{yy}$ (lower panel) as functions of charge density wave order parameter, $\psi$, for several values of $\alpha = v_F/v_\Delta$. Lines connecting the data points are guides to the eye. Note that the nodal transition at $\psi = \psi_c$ is smoothed out by increasing velocity anisotropy in a manner similar to, but distinct from, the effect of disorder.

the limit of zero temperature, as a function of $\psi$, $\Gamma_0$, and the nodal anisotropy $\alpha = v_F/v_\Delta$.

In the clean ($\Gamma_0 \to 0$), isotropic ($v_F = v_\Delta$) limit, our calculations yield a closed-form solution for the thermal conductivity tensor (plotted in Fig. 4),

$$\frac{\kappa_0^{xx}}{\kappa_{00}} = \sqrt{1 - (\psi/\psi_c)^4}\,\Theta(\psi_c - \psi), \tag{83}$$

$$\frac{\kappa_0^{yy}}{\kappa_{00}} = \frac{1 + (\psi/\psi_c)^4}{\sqrt{1 - (\psi/\psi_c)^4}}\,\Theta(\psi_c - \psi), \tag{84}$$

$$\kappa_0^{xy} = \kappa_0^{yx} = 0, \tag{85}$$

where

$$\frac{\kappa_{00}}{T} \equiv \frac{k_B^2}{3\hbar}\left(\frac{v_F}{v_\Delta} + \frac{v_\Delta}{v_F}\right), \tag{86}$$

is the zero-temperature thermal conductivity for a $d$-wave superconductor with no charge order. As expected, the thermal conductivity takes the pure $d$-wave superconductor value for $\psi = 0$ and drops to zero for $\psi > \psi_c$, where the quasiparticle energy spectrum has become fully gapped. For intermediate values of $\psi$, $\kappa_0^{xx}$ and $\kappa_0^{yy}$ differ, as square symmetry has been broken by the charge density wave. For transport in the direction of the charge density wave vector, $\kappa_0^{xx}$ vanishes continuously as $\psi$ approaches $\psi_c$. By contrast, for transport perpendicular to the charge density wave vector, $\kappa_0^{yy}$ diverges before dropping abruptly to zero at $\psi_c$. This divergence is a consequence of the clean limit and is replaced by a finite peak in the presence of disorder.

For the more complicated case of nonzero disorder ($\Gamma_0 \neq 0$) and/or anisotropic nodes ($v_F \neq v_\Delta$), we have obtained results via a numerical calculation. We find that disorder smoothes out the transition to zero thermal conductivity across the nodal collision (see Fig. 5). The clean-limit divergence in $\kappa_0^{yy}$ just before the transition is replaced by a peak which broadens and decreases in amplitude with increasing disorder. The abrupt drop in the clean-limit $\kappa_0^{xx}$ is similarly broadened. Essentially, the disorder-broadening of the quasiparticle spectral function averages over what was, in the clean limit, a sharp transition from gapless to gapped quasiparticles. We find that increased nodal anisotropy has a similar effect, amplifying the disorder effect and thereby further broadening the features in the $\psi$ dependence of the thermal conductivity (see Fig. 6). And the fact that disorder has an effect indicates that the low-temperature thermal conductivity is no longer universal (disorder-independent) in the presence of charge order, which is in line with the results of recent measurements[37–42] of low-temperature thermal transport in the underdoped cuprates, as well as other calculations.[35,48]

In these calculations, we have enjoyed the theorist's luxury of being able to turn on, by hand, a charge density wave to coexist with the $d$-wave superconductivity. The experimenter does not have direct access to such a knob. However, in the $d$-wave superconducting state of the cuprates, charge order does appear to be enhanced with underdoping. Hence the features of the $\psi$-dependent thermal conductivity curves calculated herein should serve as signatures for the underdoping-dependence of thermal conductivity measured in the underdoped cuprates. Of course, most dramatic would be the observation of the nodal collision beyond which the low-temperature thermal conductivity drops to zero. However, even if the amplitude of charge order is insufficient to reach the nodal collision, these results should provide insight to the approach to the transition.

A sequel to this work, exploring the effects of a more elaborate model of disorder, as well as the contribution of vertex corrections, is in preparation.[44] Future work will also examine the effect of different types of charge order (beyond the conventional $s$-wave case considered here) of different wave vector (beyond the unit-cell-doubling $\mathbf{Q} = (\pi/a, 0)$ case considered here) and of multiple wave vectors (such as the checkerboard charge order observed in some cuprates[22,29]).

## ACKNOWLEDGMENTS

We are grateful to S. M. Girvin, A. Abanov, and P. Schiff for very helpful discussions. This work was supported by NSF Grants No. DMR-0605919 (A.C.D.) and No. DMR-0757145 (S.S.).

## APPENDIX: SUBTLETIES OF THE SPECTRAL REPRESENTATION

In the calculations described in this paper, we have made use of the $4\times4$ extended-Nambu basis of Eq. (5) for the Hamiltonian and Green's functions. This choice of basis provides a compact realization of the Hamiltonian and is quite convenient in many respects. However, use of a matrix Green's function does introduce some subtleties regarding the spectral representation, and we would like to address those here.

All of our results could have been obtained by diagonalizing the Hamiltonian from the outset and working with the diagonalized Green's function,

$$G_D(i\omega) = U^\dagger G(i\omega) U \tag{A1}$$

with diagonal matrix elements

$$[G_D(i\omega)]_{nn} = \frac{1}{i\omega - E_k^{(n)} - \Sigma^{(n)}(i\omega)} \tag{A2}$$

where the $E_k^{(n)}$ are the eigenvalues of $H_k$, the $\Sigma^{(n)}$ are the corresponding self-energies, and the eigenvectors define the columns of unitary transformation matrix $U$. In the diagonal basis, it is quite valid to define a spectral representation for the Green's function

$$G_D(i\omega) = \int d\omega_1 \frac{A_D(\omega_1)}{i\omega - \omega_1} \tag{A3}$$

where

$$A_D(\omega) \equiv \frac{i}{2\pi}[G_D^R(\omega) - G_D^A(\omega)] = -\frac{1}{\pi}\mathrm{Im}\, G_D^R(\omega). \tag{A4}$$

Note that the second equality follows from the fact that the retarded diagonal Green's function, $G_D^R(\omega) \equiv G_D(i\omega \to \omega + i\delta)$, is the complex conjugate of the advanced diagonal Green's function, $G_D^A(\omega) \equiv G_D(i\omega \to \omega - i\delta)$, which is clear from Eq. (A2).

The non-diagonal matrix Green's function can therefore be expressed as

$$G(i\omega) = UG_D(i\omega)U^\dagger = \int d\omega_1 \frac{-\frac{1}{\pi} U\, \mathrm{Im}\, G_D^R(\omega_1) U^\dagger}{i\omega - \omega_1} \tag{A5}$$

which is not equivalent to the right-hand side of Eq. (42)

$$\int d\omega_1 \frac{-\frac{1}{\pi}\mathrm{Im}\, G^R(\omega_1)}{i\omega - \omega_1} = \int d\omega_1 \frac{-\frac{1}{\pi}\mathrm{Im}[UG_D^R(\omega_1)U^\dagger]}{i\omega - \omega_1} \tag{A6}$$

unless the diagonalization transformation commutes with taking the imaginary part. Equivalently, note that it is valid to define a non-diagonal matrix spectral function, $A(\omega) \equiv UA_D(\omega)U^\dagger$, such that

$$G(i\omega) = \int d\omega_1 \frac{A(\omega_1)}{i\omega - \omega_1} \tag{A7}$$

but

$$A(\omega) \equiv \frac{i}{2\pi}[G^R(\omega) - G^A(\omega)] \tag{A8}$$

will not be equal to $-\mathrm{Im}\, G^R/\pi$ (or even have to be real) unless the non-diagonal retarded Green's function, $G^R(\omega) \equiv G(i\omega \to \omega + i\delta)$, is the complex conjugate of the non-diagonal advanced Green's function, $G^A(\omega) \equiv G(i\omega \to \omega - i\delta)$.

For the case of real $\psi$ that we consider in this paper, $H_k$ and therefore $U$ are real, so diagonalization does commute with taking the imaginary part, $G^R$ is the complex conjugate of $G^A$, and Eq. (42) is valid. But this is not generically the case for complex $\psi$.


[1] P. A. Lee, Science **277**, 50 (1997).
[2] P. A. Lee, Phys. Rev. Lett. **71**, 1887 (1993).
[3] P. J. Hirschfeld, W. O. Putikka, and D. J. Scalapino, Phys. Rev. Lett. **71**, 3705 (1993).
[4] P. J. Hirschfeld, W. O. Putikka, and D. J. Scalapino, Phys. Rev. B **50**, 10250 (1994).
[5] P. J. Hirschfeld and W. O. Putikka, Phys. Rev. Lett. **77**, 3909 (1996).
[6] M. J. Graf, S.-K. Yip, J. A. Sauls, and D. Rainer, Phys. Rev. B **53**, 15147 (1996).
[7] T. Senthil, M. P. A. Fisher, L. Balents, and C. Nayak, Phys. Rev. Lett. **81**, 4704 (1998).
[8] A. C. Durst and P. A. Lee, Phys. Rev. B **62**, 1270 (2000).
[9] L. Taillefer, B. Lussier, R. Gagnon, K. Behnia, and H. Aubin, Phys. Rev. Lett. **79**, 483 (1997).
[10] M. Chiao, R. W. Hill, C. Lupien, B. Popic, R. Gagnon, and L. Taillefer, Phys. Rev. Lett. **82**, 2943 (1999).
[11] M. Chiao, R. W. Hill, C. Lupien, L. Taillefer, P. Lambert, R. Gagnon, and P. Fournier, Phys. Rev. B **62**, 3554 (2000).
[12] C. Proust, E. Boaknin, R. W. Hill, L. Taillefer, and A. P. Mackenzie, Phys. Rev. Lett. **89**, 147003 (2002).
[13] M. Sutherland, D. G. Hawthorn, R. W. Hill, F. Ronning, S. Wakimoto, H. Zhang, C. Proust, E. Boaknin, C. Lupien, L. Taillefer, R. Liang, D. A. Bonn, W. N. Hardy, R. Gagnon, N. E. Hussey, T. Kimura, M. Nohara, and H. Takagi, Phys. Rev. B **67**, 174520 (2003).
[14] R. W. Hill, C. Lupien, M. Sutherland, E. Boaknin, D. G. Hawthorn, C. Proust, F. Ronning, L. Taillefer, R. Liang, D. A. Bonn, and W. N. Hardy, Phys. Rev. Lett. **92**, 027001 (2004).
[15] X. F. Sun, K. Segawa, and Y. Ando, Phys. Rev. Lett. **93**, 107001 (2004).
[16] M. Sutherland, S. Y. Li, D. G. Hawthorn, R. W. Hill, F. Ronning, M. A. Tanatar, J. Paglione, H. Zhang, L. Taillefer, J. DeBenedictis, R. Liang, D. A. Bonn, and W. N. Hardy, Phys. Rev. Lett.

**94**, 147004 (2005).
[17] D. G. Hawthorn, S. Y. Li, M. Sutherland, E. Boaknin, R. W. Hill, C. Proust, F. Ronning, M. A. Tanatar, J. Paglione, L. Taillefer, D. Peets, R. Liang, D. A. Bonn, W. N. Hardy, and N. N. Kolesnikov, Phys. Rev. B **75**, 104518 (2007).
[18] X. F. Sun, S. Ono, X. Zhao, Z. Q. Pang, Y. Abe, and Y. Ando, Phys. Rev. B **77**, 094515 (2008).
[19] J. E. Hoffman, E. W. Hudson, K. M. Lang, V. Madhavan, H. Eisaki, S. Uchida, and J. C. Davis, Science **295**, 466 (2002).
[20] J. E. Hoffman, K. McElroy, D.-H. Lee, K. M. Lang, H. Eisaki, S. Uchida, and J. C. Davis, Science **297**, 1148 (2002).
[21] M. Vershinin, S. Misra, S. Ono, Y. Abe, Y. Ando, and A. Yazdani, Science **303**, 1995 (2004).
[22] T. Hanaguri, C. Lupien, Y. Kohsaka, D.-H. Lee, M. Azuma, M. Takano, H. Takagi, and J. C. Davis, Nature (London) **430**, 1001 (2004).
[23] S. Misra, M. Vershinin, P. Phillips, and A. Yazdani, Phys. Rev. B **70**, 220503(R) (2004).
[24] K. McElroy, D.-H. Lee, J. E. Hoffman, K. M. Lang, J. Lee, E. W. Hudson, H. Eisaki, S. Uchida, and J. C. Davis, Phys. Rev. Lett. **94**, 197005 (2005).
[25] Y. Kohsaka, C. Taylor, K. Fujita, A. Schmidt, C. Lupien, T. Hanaguri, M. Azuma, M. Takano, H. Eisaki, H. Takagi, S. Uchida, and J. C. Davis, Science **315**, 1380 (2007).
[26] M. C. Boyer, W. D. Wise, K. Chatterjee, M. Yi, T. Kondo, T. Takeuchi, H. Ikuta, and E. W. Hudson, Nat. Phys. **3**, 802 (2007).
[27] T. Hanaguri, Y. Kohsaka, J. C. Davis, C. Lupien, I. Yamada, M. Azuma, M. Takano, K. Ohishi, M. Ono, and H. Takagi, Nat. Phys. **3**, 865 (2007).
[28] A. N. Pasupathy, A. Pushp, K. K. Gomes, C. V. Parker, J. Wen, Z. Xu, G. Gu, S. Ono, Y. Ando, and A. Yazdani, Science **320**, 196 (2008).
[29] W. D. Wise, M. C. Boyer, K. Chatterjee, T. Kondo, T. Takeuchi, H. Ikuta, Y. Wang, and E. W. Hudson, Nat. Phys. **4**, 696 (2008).
[30] Y. Kohsaka, C. Taylor, P. Wahi, A. Schmidt, J. Lee, K. Fujita, J. W. Alldredge, K. McElroy, J. Lee, H. Eisaki, S. Uchida, D.-H. Lee, and J. C. Davis, Nature (London) **454**, 1072 (2008).
[31] S. A. Kivelson, I. P. Bindloss, E. Fradkin, V. Oganesyan, J. M. Tranquada, A. Kapitulnik, and C. Howald, Rev. Mod. Phys. **75**, 1201 (2003), and references within.
[32] K. Park and S. Sachdev, Phys. Rev. B **64**, 184510 (2001).
[33] M. Granath, V. Oganesyan, S. A. Kivelson, E. Fradkin, and V. J. Emery, Phys. Rev. Lett. **87**, 167011 (2001).
[34] M. Vojta, Y. Zhang, and S. Sachdev, Phys. Rev. B **62**, 6721 (2000).
[35] V. P. Gusynin and V. A. Miransky, Eur. Phys. J. B **37**, 363 (2004).
[36] E. Berg, C.-C. Chen, and S. A. Kivelson, Phys. Rev. Lett. **100**, 027003 (2008).
[37] J. Takeya, Y. Ando, S. Komiya, and X. F. Sun, Phys. Rev. Lett. **88**, 077001 (2002).
[38] X. F. Sun, S. Komiya, J. Takeya, and Y. Ando, Phys. Rev. Lett. **90**, 117004 (2003).
[39] Y. Ando, S. Ono, X. F. Sun, J. Takeya, F. F. Balakirev, J. B. Betts, and G. S. Boebinger, Phys. Rev. Lett. **92**, 247004 (2004).
[40] X. F. Sun, K. Segawa, and Y. Ando, Phys. Rev. B **72**, 100502(R) (2005).
[41] X. F. Sun, S. Ono, Y. Abe, S. Komiya, K. Segawa, and Y. Ando, Phys. Rev. Lett. **96**, 017008 (2006).
[42] D. G. Hawthorn, R. W. Hill, C. Proust, F. Ronning, M. Sutherland, E. Boaknin, C. Lupien, M. A. Tanatar, J. Paglione, S. Wakimoto, H. Zhang, L. Taillefer, T. Kimura, M. Nohara, H. Takagi, and N. E. Hussey, Phys. Rev. Lett. **90**, 197004 (2003).
[43] C. Nayak, Phys. Rev. B **62**, 4880 (2000).
[44] P. R. Schiff and A. C. Durst, Physica C **469**, 740 (2009).
[45] G. D. Mahan, *Many-Particle Physics* (Plenum, New York, 1990).
[46] V. Ambegaokar and A. Griffin, Phys. Rev. **137**, A1151 (1965).
[47] I. S. Gradshteyn and I. M. Ryzhik, *Table of Integrals, Series, and Products* (Academic Press, San Diego, 1994).
[48] B. M. Andersen and P. J. Hirschfeld, Phys. Rev. Lett. **100**, 257003 (2008).